Cancer Cell
Article

A High-Frequency Regulatory Polymorphism in the p53 Pathway Accelerates Tumor Development

Sean M. Post,[1] Alfonso Quintás-Cardama,[1,2] Vinod Pant,[1] Tomoo Iwakuma,[5] Amir Hamir,[3] James G. Jackson,[1] Daniela R. Maccio,[1] Gareth L. Bond,[6] David G. Johnson,[4] Arnold J. Levine,[7] and Guillermina Lozano[1,*]
[1]Department of Genetics
[2]Department of Leukemia
[3]Department of Veterinary Medicine and Surgery
[4]Department of Carcinogenesis
The University of Texas M.D. Anderson Cancer Center, Houston, TX 77030, USA
[5]Louisiana State University Health Sciences Center, Department of Genetics/Cancer Center, New Orleans, LA, 70112, USA
[6]Ludwig Institute for Cancer Research, University of Oxford, Oxford, OX1 3DW, UK
[7]The Simons Center for Systems Biology, The Institute for Advanced Study, Princeton, NJ 08540, USA
*Correspondence: gglozano@mdanderson.org
DOI 10.1016/j.ccr.2010.07.010

SUMMARY

MDM2, a negative regulator of p53, is elevated in many cancers that retain wild-type *p53*. A single nucleotide polymorphism (SNP) in the human *MDM2* promoter increases the affinity of Sp1 resulting in elevated MDM2 levels. We generated mice carrying either the $MDM2^{SNP309T}$ or the $MDM2^{SNP309G}$ allele to address the impact of $MDM2^{SNP309G}$ on tumorigenesis. $Mdm2^{SNP309G/G}$ cells exhibit elevated Mdm2 levels, reduced p53 levels, and decreased apoptosis. Importantly, some $Mdm2^{SNP309G/G}$ mice succumbed to tumors before 1 year of age, suggesting that this allele increases tumor risk. Additionally, the $Mdm2^{SNP309G}$ allele potentiates the tumor phenotype and alters tumor spectrum in mice inheriting a p53 hot-spot mutation. These data provide causal evidence for increased cancer risk in carriers of the $Mdm2^{SNP309G}$ allele.

INTRODUCTION

Ablation of the p53 tumor suppressor pathway is a hallmark of tumorigenesis as evidenced by the fact that p53 is the most commonly mutated or inactivated tumor suppressor in neoplastic malignancies. *p53* encodes a transcription factor that activates numerous cell cycle arrest, senescence, and apoptotic genes (Vogelstein et al., 2000). Mutations in or deletions of the *p53* gene occur in >50% of human cancers (Soussi and Lozano, 2005). In cancers lacking p53 mutations, other components of the p53 pathway are altered during tumorigenesis, contributing to the functional inactivation of the p53 pathway (Soussi and Lozano, 2005). Most notably, the *MDM2* gene is amplified in >30% of sarcomas and the MDM2 protein is overexpressed in multiple human cancers that retain wild-type *p53* (Oliner et al., 1992; Valentin-Vega et al., 2007). *Mdm2* is a protooncogene that encodes an E3 ubiquitin ligase that negatively regulates p53 protein stability and transcriptional activity (Iwakuma and Lozano, 2003). These data underscore the fact that decreased levels of p53, resulting from mutations in the p53 gene or alterations in the stoichiometry of its inhibitor MDM2 play a critical role during tumor development.

A T-to-G single nucleotide polymorphism (SNP) in the second promoter (P2) of the human *MDM2* gene (SNP309G) has been identified (Bond et al., 2004). This SNP is present in the heterozygous state (G/T) in ~40% and in the homozygous state (G/G) in 15% of healthy individuals, respectively (Bond et al., 2006). $MDM2^{SNP309G}$ enhances the binding of the transcriptional

Significance

Proper regulation of the homeostatic balance between p53 and Mdm2 is critical in tumorigenesis. The identification of the polymorphic $MDM2^{SNP309G}$ allele in humans, which alters this delicate balance, has lead to an intense focus on the impact of this SNP in accelerating tumorigenesis. There have been numerous conflicting reports regarding the importance of this SNP in the clinic. To directly assess the impact of $Mdm2^{SNP309}$, we generated cohorts of mice that either carry the polymorphic $Mdm2^{SNP309G}$ or $Mdm2^{SNP309T}$ alleles and monitored these mice for tumor development. Mice harboring two $Mdm2^{SNP309G}$ alleles have an attenuated p53 pathway resulting in a shorter latency to tumor formation and decreased survival. These results demonstrate the $Mdm2^{SNP309G}$ allele has a direct impact on cancer risk.

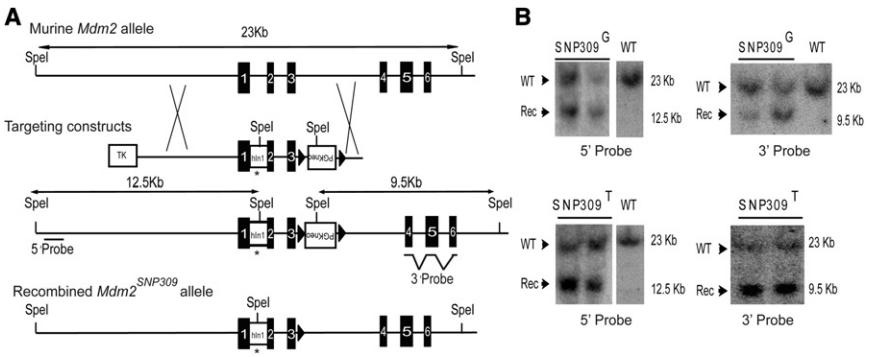

Figure 1. Generation of Mice Containing Either the Humanized *Mdm2*^{SNP309G} or *Mdm2*^{SNP309T} Allele

(A) The targeting vectors were designed to incorporate the *PGK-neo* selectable marker in intron 3 flanked by *loxP* sites (triangles) containing the entire human intron 1 (hIn1) with a G or T nucleotide at SNP309 (denoted by an asterisk). Black numbered boxes denote *Mdm2* exons. After Cre-mediated recombination, the *PGK-neo* cassette was deleted.

(B) Southern blot analysis of *SpeI*-digested DNA from ES cell clones electroporated with the *Mdm2*^{SNP309G} or the *Mdm2*^{SNP309T} targeting vectors. The 23-kb *SpeI* fragment represents the wild-type *Mdm2* allele whereas the 12.5-kb *SpeI* fragment is the expected size for the recombined allele using a 5′ probe. Wild-type (WT) DNA serves as a control. The 9.5-kb *SpeI* fragment is the expected size for the recombined alleles using a 3′ probe. See also Figure S1.

activator Sp1 to the P2 promoter of *MDM2* resulting in a constitutive increase in *MDM2* transcription. This in turn leads to increased levels of the MDM2 protein and therefore decreased p53 protein levels. Most importantly, the *MDM2*^{SNP309G} allele has been associated with an increased cancer risk in some human tumors that express wild-type p53 (Bond et al., 2006; Dharel et al., 2006; Grochola et al., 2010; Yarden et al., 2008). However, a significant number of reports have failed to corroborate such a notion (Krekac et al., 2008; Khan et al., 2008). Clinical correlates aimed at supporting the effect of the *MDM2*^{SNP309G} allele in humans with spontaneous cancers have been controversial, likely as a result of the heterogeneity of the employed data sets and the retrospective nature of these analyses (Bond et al., 2006; Bond and Levine, 2007; Copson et al., 2006; Dharel et al., 2006; Economopoulos and Sergentanis, 2009; Ellis et al., 2008; Grochola et al., 2010; Menin et al., 2006; Schmidt et al., 2007; Yarden et al., 2008).

Additional support of an enhanced cancer risk in *MDM2*^{SNP309} carriers is the fact that patients diagnosed with Li-Fraumeni syndrome (LFS) with an inherited germline mutation in *p53* and homozygous for the G nucleotide at *MDM2*^{SNP309}develop tumors approximately 10 years earlier than LFS patients lacking this polymorphism (Bond et al., 2004; Bougeard et al., 2006; Marcel et al., 2009; Ruijs et al., 2007; Tabori et al., 2007). Additionally, patients with LFS carrying two *MDM2*^{SNP309G} alleles are more frequently diagnosed with multiple primary tumors compared to LFS patients carrying two *MDM2*^{SNP309T} alleles. Together, these data suggest an enhanced cancer phenotype in patients carrying germline-inactivating mutations in *p53* and *MDM2*^{SNP309G}. Thus, increased MDM2 levels resulting from the presence of the *MDM2*^{SNP309G} allele may further down modulate an already muted p53 pathway. These data are however correlative by nature.

Recent attempts to understand the mechanisms that regulate the Mdm2-p53 pathway during tumorigenesis have focused on the generation of mouse models that genetically delete *p53*, overexpress genes that regulate p53, or produce mutant p53 proteins that mimic human mutations (Donehower and Lozano, 2009). Additionally, though, more subtle changes also affect tumorigenesis. For example, haploinsufficiency at the *Mdm2* locus delays tumor onset in mice carrying an *Eμ-myc* transgene and also renders mice sensitive to DNA damage (Alt et al., 2003; Mendrysa et al., 2003; Terzian et al., 2007). However, little is known about the impact of more subtle genetic modifiers that affect the regulation or expression of proteins involved in tumorigenesis. In this study, we have used the naturally occurring polymorphism in the *MDM2* promoter to generate two humanized *Mdm2*^{SNP309} murine alleles to examine the direct impact of this polymorphism on tumor development.

RESULTS

Generation of *Mdm2*^{SNP309} Mice

To directly test the significance of *Mdm2*^{SNP309} in a prospective manner, we generated humanized *Mdm2*^{SNP309} alleles in the mouse. Using a PCR-based strategy, we generated *Mdm2*^{SNP309G} and *Mdm2*^{SNP309T} targeting constructs by replacing the mouse intron 1 (containing the entire P2 promoter) with the corresponding human intron 1 with either the G or T polymorphism. Both targeting constructs were sequenced in their entirety to rule out the presence of additional changes. *MDM2*^{SNP309G} and *MDM2*^{SNP309T} human intron 1 sequences are identical, except for the polymorphism (Figure S1A available online). The polymorphisms were introduced into the murine *Mdm2* locus by homologous recombination in embryonic stem (ES) cells (Figure 1A). Southern blot analysis of the recombination event revealed correct targeting of both constructs at the murine *Mdm2* locus (Figure 1B). Additionally, Southern blot analysis using a probe against the neomycin cassette verified single copy integration and indicated the absence of other insertions (Figures S1B and S1C). Chimeric mice were backcrossed with C57Bl/6 mice for five generations, including one cross with *Zp3-Cre* mice (also in a C57Bl/6 background) that resulted in Cre-loxP-mediated excision of the PGK-neomycin cassette. A cohort of *Mdm2*$^{SNP309G/G}$ and *Mdm2*$^{SNP309T/T}$ mice was established for tumor studies. The background of all mice used in these studies is >98% C57Bl/6.

Mdm2 mRNA Levels Are Increased in Tissues from *Mdm2*$^{SNP309G/G}$ Mice

To characterize the polymorphic alleles, we first measured the total level of *Mdm2* mRNA in *Mdm2*^{SNP309} mice. Real-time RT-PCR revealed that the spleens and thymi (two p53 sensitive tissues) of 6-week-old *Mdm2*$^{SNP309G/G}$ mice had significantly higher levels of *Mdm2* mRNA (2.08 ± 0.37 and 3.7 ± 1.1, spleens and thymi, respectively) as compared to the control

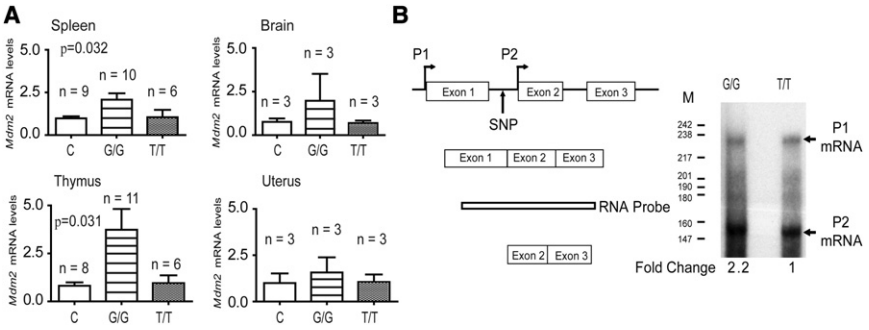

Figure 2. $Mdm2^{SNP309G/G}$ Mice Have Higher Levels of *Mdm2* mRNA as Compared to $Mdm2^{SNP309T/T}$ and C57Bl/6 Mice

(A) Real-time RT-PCR analysis for *Mdm2* mRNA levels in spleen, brain, thymus, and uterus of C57Bl/6 (C), $Mdm2^{SNP309G/G}$ (G/G), and $Mdm2^{SNP309T/T}$ (T/T) mice. The mean and standard error of the mean (SEM) were determined from triplicate samples after normalization to *Rplp0* for the number (n) of mice indicated. Statistical significance in the spleen ($p = 0.032$) and thymus ($p = 0.031$) was determined by one-way analysis of variance (ANOVA).

(B) RNase protection analysis for *Mdm2* mRNA levels in spleen of $Mdm2^{SNP309G/G}$ and $Mdm2^{SNP309T/T}$ mice. Schematic of the *Mdm2* locus and RNase protection probe. P1 (transcript from promoter 1), upper band and P2 (transcript from promoter 2), lower band. Fold change was determined by calculating the ratios of P2/P1 in each sample. See also Figure S2.

$Mdm2^{SNP309T/T}$ (1.05 ± 0.43 and 0.95 ± 0.41, spleens and thymi, respectively) and wild-type C57Bl/6 (that carry the endogenous murine intron 1) (0.98 ± 0.12 and 0.81 ± 0.18, spleens and thymi, respectively) mice. The levels of *Mdm2* in the $Mdm2^{SNP309G/G}$ tissues were significantly higher than in control mice ($p = 0.032$ and $p = 0.031$, spleen and thymus respectively, one-way analysis of variance [ANOVA]) (Figure 2A). Likewise, the brains and uteri of 6-week-old $Mdm2^{SNP309G/G}$ mice had higher levels of *Mdm2*, although not statistically significant, as compared to control mice (Figure 2A). RNase protection assays were subsequently used to quantitate and distinguish the otherwise identical transcripts arising from the basal (P1) and P2 promoters (the second promoter that has the $MDM2^{SNP309}$). Data show a 2.2-fold increase in *Mdm2* levels from the P2 promoter in spleens taken from $Mdm2^{SNP309G/G}$ mice as compared to those obtained from $Mdm2^{SNP309T/T}$ mice (Figure 2B). The levels of *Mdm2* mRNA from the P1 promoter were unchanged in both $Mdm2^{SNP309G/G}$ and $Mdm2^{SNP309T/T}$ mice (Figure 2B). These data were further validated using real time RT-PCR primers specific to the transcript generated from the P1 promoter. No significant difference was noted in the levels of P1 *Mdm2* mRNA in C57Bl/6 (0.86 ± 0.12), $Mdm2^{SNP309G/G}$ (1.16 ± 0.28), and $Mdm2^{SNP309T/T}$ (1.16 ± 0.15) mice (ANOVA, $p = 0.469$; Figure S2). These data indicate that the increased levels of *Mdm2* in vivo are specifically due to the presence of $Mdm2^{SNP309G}$ in the P2 promoter.

Mdm2 Levels in $Mdm2^{SNP309G/G}$ Mouse Embryonic Fibroblasts Are Sensitive to the Sp1 Inhibitor Mithramycin A

In humans cell lines the $MDM2^{SN309}$ polymorphism creates a stable binding site for the transcription factor Sp1 (Bond et al., 2004). Mithramycin A disrupts the activity of Sp1, and treatment of $MDM2^{SNP309G/G}$ human cells with mithramycin A resulted in a decrease in Mdm2 levels (Bond et al., 2004; Chien et al., 2010). We therefore assessed the impact of mithramycin A on *Mdm2* mRNA and protein levels. The levels of *Mdm2* were significantly reduced in $Mdm2^{SNP309G/G}$ mouse embryo fibroblasts (MEFs) on mithramycin A treatment (0.98 ± 0.03 and 0.19 ± 0.18, untreated versus treated, respectively, $p < 0.0001$) (Figure 3A). Western blot analysis revealed that $Mdm2^{SNP309G/G}$ MEFs had lower levels of Mdm2 protein after mithramycin A treatment (Figure 3B). Mithramycin A did not significantly alter the levels of *Mdm2* in $Mdm2^{SNP309T/T}$ MEFs, although the *Mdm2* levels in the untreated $Mdm2^{SNP309T/T}$ MEFs were much lower than the untreated $Mdm2^{SNP309G/G}$ MEFs (Figure 3A and B). Thus, although the basal levels of

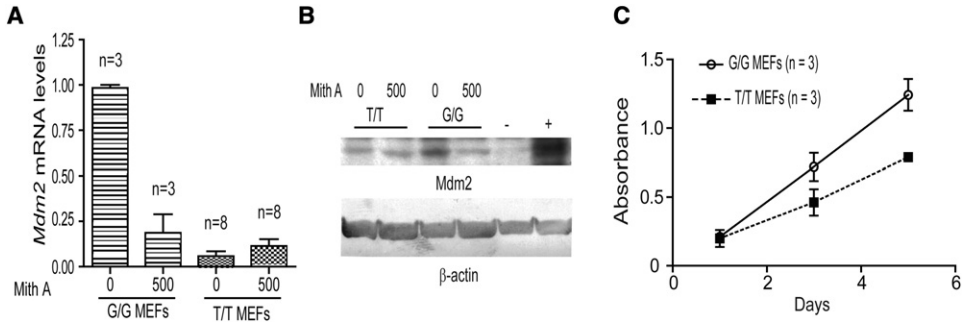

Figure 3. *Mdm2* Levels Are Higher in $Mdm2^{SNP309G/G}$ Mouse Embryonic Fibroblasts as Compared to $Mdm2^{SNP309T/T}$ and C57Bl/6 Fibroblasts

(A) Real time RT-PCR analysis for transcriptional activation of *Mdm2* in $Mdm2^{SNP309G/G}$ and $Mdm2^{SNP309T/T}$ mouse embryo fibroblasts (MEFs) isolated from at least three separate embryos per genotype. MEFs were either untreated or treated with 500nM mithramycin A for 18 hr. The mean and standard error of the mean (SEM) were determined from triplicate samples after normalization to *Rplp0* for the number (n) of different MEF lines indicated.

(B) Western blots of untreated or 500 nM mithramycin A-treated $Mdm2^{SNP309G/G}$ and $Mdm2^{SNP309T/T}$ lysates were carried out and blotted with Mdm2 and β-actin antibodies. Lysates from IR treated *Mdm2*-transgenic (+) and $Mdm2^{-/-}$ $p53^{-/-}$ MEFs (–) serve as positive and negative controls, respectively.

(C) Cell proliferation rates of $Mdm2^{SNP309G/G}$ and $Mdm2^{SNP309T/T}$ MEFs. Three separate low passage (P2) MEF cell lines per genotype were plated, grown for 1, 3, or 5 days, and then assayed for cell number. Each data point represents the mean and SEM for three separate MEF lines per genotype.

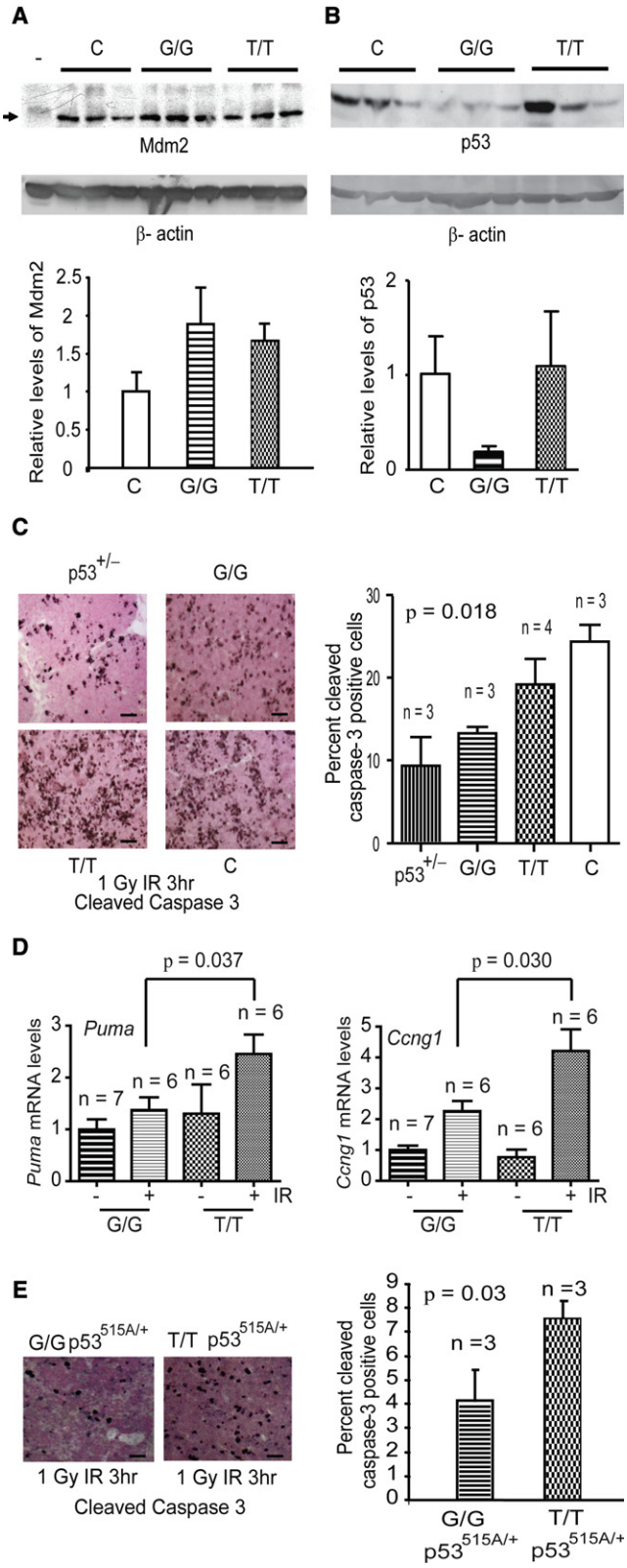

Figure 4. The *Mdm2*^{SNP309G} Allele Results in Reduced p53 Activity

(A) Western blots of C57Bl/6 (C), *Mdm2*$^{SNP309G/G}$ (G/G), and *Mdm2*$^{SNP309T/T}$ (T/T) splenic lysates were performed and blotted with Mdm2 and β-actin antibodies. *Mdm2*$^{-/-}$ *p53*$^{-/-}$ splenic lysates (–) serve as an Mdm2 negative control. The mean and SEM of the three control samples was determined by the ratio between the Mdm2 bands and the corresponding β-actin bands and arbitrarily set to one. The mean and SEM of Mdm2 in splenic lysates from *Mdm2*$^{SNP309G/G}$ and *Mdm2*$^{SNP309T/T}$ mice was determined by comparing the ratios of Mdm2/β-actin normalized to the control ratio.

(B) Western blots of C57Bl/6 (C), *Mdm2*$^{SNP309G/G}$ (G/G), and *Mdm2*$^{SNP309T/T}$ (T/T) lysates were carried out and blotted with p53 and β-actin antibodies. The mean and SEM was determined as above.

(C) Apoptosis was determined by counting the percentage of cleaved caspase-3 positive cells in the thymi of *p53*$^{+/-}$ (9.1% ± 3.5%), *Mdm2*$^{SNP309G/G}$ (G/G) (13.3% ± 0.77%), *Mdm2*$^{SNP309T/T}$ (T/T) (19.0% ± 3.1%), and C57Bl/6 (C) (24.3% ± 2.0%) mice after 1 Gy ionizing radiation (IR). At least 300 cells were counted from three randomized high magnification fields per animal. The mean and SEM for each genotype were calculated from at least three thymi per genotype. Statistical significance was determined by one-way ANOVA. n = the number of mice examined for each genotype. The scale bar represents 50 μm.

(D) Real-time RT-PCR analysis for mRNA levels of the p53-dependent targets *Puma* and *Ccng1* in the thymus of untreated (–) *Mdm2*$^{SNP309G/G}$ (G/G) and *Mdm2*$^{SNP309T/T}$ (T/T) mice or *Mdm2*$^{SNP309G/G}$ (G/G) and *Mdm2*$^{SNP309T/T}$ (T/T) mice treated (+) with 1 Gy ionizing radiation. Thymi were harvested from irradiated mice 3 hr posttreatment. The mean and SEM were determined from triplicate samples after normalization to *Rplp0* for the number (n) of mice indicated. Statistical significance was determined by unpaired Student's t test.

(E) Apoptosis was determined by counting the percentage of cleaved caspase-3 positive cells in *Mdm2*$^{SNP309T/T}$ *p53*$^{515A/+}$ and *Mdm2*$^{SNP309G/G}$ *p53*$^{515A/+}$ thymi. At least 300 cells were counted from three high magnification fields per thymus per genotype. The mean and SEM of each genotype were calculated from three separate mice. Statistical significance was determined by unpaired Student's t test. n = the number of mice examined for each genotype. The scale bar represents 50 μm. See also Figure S3.

Mdm2 were dramatically different in fibroblasts, mithramycin A decreased expression of *Mdm2* only in *Mdm2*$^{SNP309G/G}$ MEFs.

Given the differences in Mdm2 levels between the *Mdm2*$^{SNP309G/G}$ and *Mdm2*$^{SNP309T/T}$ MEFs, we tested whether these differences conferred a growth advantage. We found that the *Mdm2*$^{SNP309G/G}$ MEFs had an increased rate of proliferation as compared to the *Mdm2*$^{SNP309T/T}$ MEFs, with a slope of 0.26 ± 0.029 and 0.15 ± 0.022, respectively (Figure 3C). Thus early passage *Mdm2*$^{SNP309G/G}$ MEFs have a growth advantage as compared to the *Mdm2*$^{SNP309T/T}$ MEFs.

The p53 Pathway Is Partially Attenuated in *Mdm2*$^{SNP309G/G}$ Mice

It is widely appreciated that Mdm2 levels tightly control p53 levels in vivo (Iwakuma and Lozano, 2003). To determine how small increases in *Mdm2* levels impact the p53 pathway, we first examined the levels of Mdm2 and p53 protein in mouse tissues. Spleens from *Mdm2*$^{SNP309G/G}$ mice had elevated levels of Mdm2 protein and consequently lower levels of p53 as compared to control *Mdm2*$^{SNP309T/T}$ and wild-type C57Bl/6 mice (Figures 4A and 4B). To test the functional consequences of lower levels of p53 in mice harboring the *Mdm2*^{SNP309G} allele, *Mdm2*$^{SNP309G/G}$, *Mdm2*$^{SNP309T/T}$, *p53*$^{+/-}$, and C57Bl/6 mice were exposed to low dose (1 Gy) ionizing radiation (IR). This dose of IR triggers a robust p53 response in the thymus (Alvarez et al., 2006). Thymi from *Mdm2*$^{SNP309G/G}$ mice exhibited a significantly lower apoptotic response after low dose IR (13.3 ± 0.77% cleaved caspase-3 positive cells) as compared to the *Mdm2*$^{SNP309T/T}$ (19.0% ± 3.1% cleaved caspase-3 positive cells) or wild-type C57Bl/6 (24.3 ± 2.0% cleaved caspase-3 positive cells) mice

(Figure 4C, ANOVA, p = 0.018). In fact, the levels of p53-dependent apoptosis in $Mdm2^{SNP309G/G}$ thymi were comparable to *p53* heterozygous mice (p = 0.304). These data suggest that the presence of two $Mdm2^{SNP309G}$ alleles significantly inhibited p53-dependent apoptosis in response to DNA damage. To examine the activation of downstream effectors of p53 function, we quantified activation of apoptotic and cell cycle arrest transcriptional targets of p53 after IR. The pro-apoptotic factor, *Puma*, and the cell cycle inhibitor, *Ccng1* (the gene that codes for Cyclin G1), were significantly lower in thymi from irradiated $Mdm2^{SNP309G/G}$ mice as compared to thymi from irradiated $Mdm2^{SNP309T/T}$ mice, (p = 0.037 and p = 0.030, respectively) (Figure 4D). Two other p53 targets, *Pig8* and *p21*, were decreased in thymi isolated from irradiated $Mdm2^{SNP309G/G}$ mice; however, neither reached statistical significance (Figure S3A). These data suggest that the presence of the $Mdm2^{SNP309G}$ allele attenuates activation of the p53 pathway in the thymus after low dose irradiation.

To explore the impact of the $Mdm2^{SNP309G}$ allele on other tissues exposed to low dose IR, we collected epithelial tissues from these mice. Several transcriptional targets of p53 were modestly attenuated in the intestine and breast (female) of $Mdm2^{SNP309G/G}$ mice, specifically *Puma* in intestine and *p21* in breast, as compared to the $Mdm2^{SNP309T/T}$ mice after low dose IR; however, transactivation of no gene reached statistical significance (Figures S3B and S3C). These results suggest that either epithelial tissues are less sensitive to low dose IR or that transactivation of p53 targets is tissue specific after exposure to IR. Lastly, we measured p53 protein levels and phosphorylation in different tissues after low dose IR. $Mdm2^{SNP309G/G}$ thymus and breast tissues show lower basal levels of p53 (Figures S3D and S3E), consistent with our observation of low basal p53 levels in the $Mdm2^{SNP309G/G}$ spleens (Figure 4B). No statistically significant differences were observed in p53 levels 3 hr post-IR (Figures S3F and S3G). Together, these findings suggest that after IR the polymorphic $Mdm2^{SNP309}$ allele has a more prominent impact on p53 activity rather than on p53 stability.

We also examined the impact of $Mdm2^{SNP309G/G}$ on apoptosis in a mutant *p53* background by crossing the $Mdm2^{SNP309}$ mice with mice carrying the $p53^{515A}$ hot-spot mutation that encodes the p53R172H mutant protein (Lang et al., 2004). Thymi from $Mdm2^{SNP309G/G}$ $p53^{515A/+}$ mice also had a significant reduction in apoptotic cells as compared to the control $Mdm2^{SNP309T/T}$ $p53^{515A/+}$ mice after low dose IR (p = 0.03) (Figure 4E). These data suggest that mice harboring two $Mdm2^{SNP309G}$ alleles have a diminished p53 response after DNA damage both in wild-type and heterozygous mutant p53 backgrounds.

$Mdm2^{SNP309G}$ Allele Resulted in Increased Cancer Risk

To investigate the impact of $Mdm2^{SNP309G/G}$ on cancer risk in vivo we monitored cohorts of $Mdm2^{SNP309G/G}$, $Mdm2^{SNP309T/T}$, $Mdm2^{SNP309G/G}$ $p53^{515A/+}$, $Mdm2^{SNP309T/T}$ $p53^{515A/+}$, and $p53^{515A/+}$ mice for tumor formation. Tumor burdened and moribund mice of each genotype were sacrificed and tumors were harvested for pathological analysis. The overall survival of $Mdm2^{SNP309G/G}$ mice was reduced as compared to the $Mdm2^{SNP309T/T}$ mice (p = 0.015) (Figure 5A). Five of ten $Mdm2^{SNP309G/G}$ mice and one of five $Mdm2^{SNP309T/T}$ mice that died had obvious tumor involvement (Table 1). Several $Mdm2^{SNP309G/G}$ and $Mdm2^{SNP309T/T}$ mice died of unknown causes. $Mdm2^{SNP309G/G}$ $p53^{515A/+}$ mice also succumbed to tumors significantly earlier than the $Mdm2^{SNP309T/T}$ $p53^{515A/+}$ and $p53^{515A/+}$ mice (p = 0.0005) (Figure 5B). The median overall survival for the $Mdm2^{SNP309G/G}$ $p53^{515A/+}$ and $Mdm2^{SNP309T/T}$ $p53^{515A/+}$ cohorts was 401 and 482 days, respectively (hazard ratio = 0.561; confidence interval = 0.408–0.786). These results indicate that the $Mdm2^{SNP309G}$ allele directly increases cancer risk.

$Mdm2^{SNP309G}$ Impacts the Mdm2-p53 Axis in Tumors

To explore the molecular events that occur during tumor formation, we investigated the status of Mdm2 and p53. Immunohistochemical analysis of Mdm2 in tumors isolated from the $Mdm2^{SNP309}$ mice showed 48% (10 of 21) of $Mdm2^{SNP309G/G}$ $p53^{515A/+}$ tumors expressed Mdm2, whereas only 17% (3 of 18) $Mdm2^{SNP309T/T}$ $p53^{515A/+}$ tumors expressed Mdm2 (p = 0.041, Figure 5C). Because cells exert tremendous selective pressure to delete wild-type p53 function during tumorigenesis, we also tested whether these tumors underwent loss of heterozygosity (LOH) of the remaining wild-type *p53* allele. Notably, 32% (10 of 31) of $Mdm2^{SNP309G/G}$ $p53^{515A/+}$ tumors retained the wild-type *p53* allele compared to only 19% (5 of 26) of $Mdm2^{SNP309T/T}$ $p53^{515A/+}$ tumors, although these data were not statistically significant (Figure 5C). Western blot analysis revealed that all but one tumor (12 of 13) that retained the wild-type *p53* allele expressed p53, regardless of genotype (Figure S4A). Additionally, p53 was phosphorylated in all the tumors that retained both *p53* alleles (Figure S4A). In tumors with LOH of the wild-type *p53* allele, 60% (3 of 5) of the $Mdm2^{SNP309G/G}$ $p53^{515A/+}$ tumors expressed mutant p53 and 100% (6 of 6) of the $Mdm2^{SNP309T/T}$ $p53^{515A/+}$ tumors expressed high levels of mutant p53 (Figure S6B). Furthermore, 40% (2 of 5) of the $Mdm2^{SNP309G/G}$ $p53^{515A/+}$ tumors had high levels of phosphorylated mutant p53, whereas 67% (4 of 6) of the $Mdm2^{SNP309T/T}$ $p53^{515A/+}$ tumors expressed phosphorylated mutant p53 (Figure S4B).

An examination of p53 targets in tumors revealed that mRNA levels of p53 targets varied greatly in each tumor, likely as a consequence of multiple additional genetic alterations occurring during tumorigenesis. However, one p53-dependent pro-apoptotic target, *Perp*, was significantly attenuated in the tumors for the $Mdm2^{SNP309G/G}$ $p53^{515A/+}$ mice as compared to tumors from the $Mdm2^{SNP309T/T}$ $p53^{515A/+}$ mice (p = 0.023; Figure S4C).

$Mdm2^{SNP309G}$ Alters Tumor Spectrum

In addition to accelerated tumor onset, $Mdm2^{SNP309G/G}$ and $Mdm2^{SNP309G/G}$ $p53^{515A/+}$ mice also developed tumor types only anecdotally reported in C57Bl/6 or $p53^{515A}$ mice. One $Mdm2^{SNP309G/G}$ mouse developed a mammary adenocarcinoma in addition to a lymphoma (Figures 6 A–6D, and Table 1). Three $Mdm2^{SNP309G/G}$ $p53^{515A/+}$ mice developed mammary adenocarcinomas (Figures 6 E–I and Table 1), and one developed a squamous cell papilloma (Figure 6G). Because mammary adenocarcinomas have never been detected in our *p53* cohorts in a C57Bl/6 background, we confirmed the breast origin of these tumors by demonstrating the expression of the estrogen receptor-α (Figures 6D and 6I). Additionally and similar to patients with LFS that harbor two $Mdm2^{SNP309G}$ alleles (Bond et al., 2004), $Mdm2^{SNP309G/G}$ $p53^{515A/+}$ mice also developed

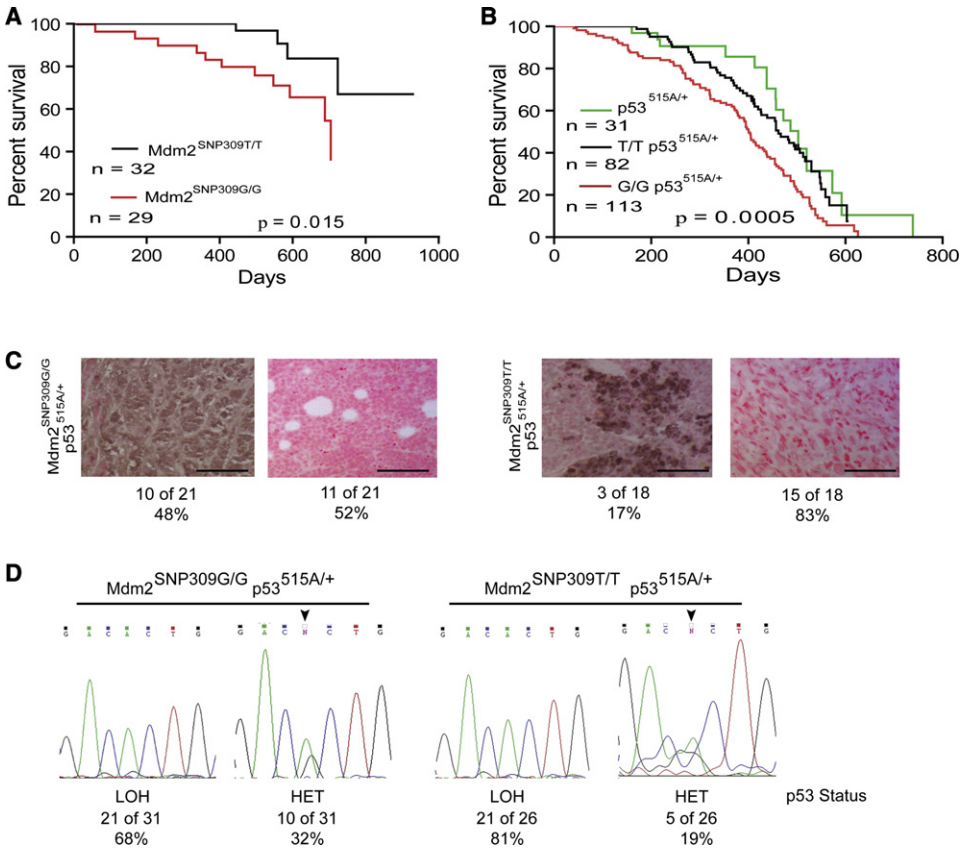

Figure 5. Mice Harboring Two *Mdm2*^{SNP309G} Alleles have Decreased Survival as Compared to Mice Possessing Two *Mdm2*^{SNP309T} Alleles

(A) Kaplan-Meier curves indicating survival of *Mdm2*$^{SNP309T/T}$ and *Mdm2*$^{SNP309G/G}$ mice. Statistical significance was determined by log rank test.

(B) Kaplan-Meier curves indicating the survival of *p53*$^{515A/+}$, *Mdm2*$^{SNP309T/T}$ *p53*$^{515A/+}$, or *Mdm2*$^{SNP309G/G}$ *p53*$^{515A/+}$ mice. Statistical significance was determined by log rank test.

(C) Mdm2 expression in tumors from *Mdm2*$^{SNP309G/G}$ *p53*$^{515A/+}$ and *Mdm2*$^{SNP309T/T}$ *p53*$^{515A/+}$ mice. Forty-eight percent (10 of 21) of tumors from *Mdm2*$^{SNP309G/G}$ *p53*$^{515A/+}$ mice and 17% (3 of 15) *Mdm2*$^{SNP309T/T}$ *p53*$^{515A/+}$ mice express Mdm2 ($p = 0.041$). Statistical significance was determined by the χ^2 test. Tumor sections were considered positive if >10% of the total cells were immunoreactive for Mdm2. The scale bar represents 100 μm.

(D) Loss of heterozygosity (LOH) varies at the *p53* locus in *Mdm2*$^{SNP309G/G}$ *p53*$^{515A/+}$ and *Mdm2*$^{SNP309T/T}$ *p53*$^{515A/+}$ tumors. Exon 5, containing the *p53*^{515A} mutation, was sequenced in 31 *Mdm2*$^{SNP309G/G}$ *p53*$^{515A/+}$ and 26 *Mdm2*$^{SNP309T/T}$ *p53*$^{515A/+}$ tumors, respectively. LOH was determined by a >50% reduction of the wild-type allele, noted by the absence of the G nucleotide at position 515. HET denotes retention of both p53 alleles. See also Figure S4.

multiple primary tumors as compared to *Mdm2*$^{SNP309T/T}$ *p53*$^{515A/+}$ mice (Figure 6L), recapitulating the human phenotype.

DISCUSSION

The sequencing of the human genome has unveiled the presence of millions of SNPs (Venter et al., 2001). Deciphering the effects of individual SNPs in human cancer has proven extremely challenging given the multitude of SNPs, the number of redundant and overlapping pathways they intersect with, and the heterogeneous genetic make-up of humans. Since the identification of the *Mdm2*^{SNP309} allele, multiple studies involving large numbers of patients diagnosed with cancer have suggested that the *Mdm2*^{SNP309G} allele significantly increases cancer risk, whereas other studies have failed to show such an association. For less common cancers, such as leukemia, ovarian cancer, lymphoma, or melanoma, the impact of *Mdm2*^{SNP309} is even less clear given the retrospective nature of these studies and the small size of the cohorts analyzed.

To determine the direct impact of this SNP in tumorigenesis, we generated two genetically engineered mouse models carrying either *Mdm2*^{SNP309G} or *Mdm2*^{SNP309T} alleles and followed both cohorts of animals, prospectively. A critical advantage of this mouse model is that we have controlled for the cancer phenotype variability that arises from environmental, stochastic, and modifier gene effects as these mice are >96% C57Bl/6 and, therefore, isogeneic. Mice carrying two *Mdm2*^{SNP309G} alleles had increased levels of Mdm2 mRNA and protein, decreased p53 levels, and a marked attenuation of the p53 response after ionizing radiation as compared to *Mdm2*$^{SNP309T/T}$ or wild-type C57Bl/6 mice. Our findings suggest that the presence of the *Mdm2*^{SNP309G} allele contributes to accelerated tumor formation and reduction in overall survival in mice that harbor either wild-type or mutant *p53*. The observation that the *Mdm2*^{SNP309G} allele alone is sufficient to cause an increased cancer risk in our mouse models supports the retrospective studies associating the *MDM2*^{SNP309G} allele with enhanced tumorigenesis in humans.

Table 1. Tumor Spectrum of $Mdm2^{SNP309G/G}$, $Mdm2^{SNP309T/T}$, $Mdm2^{SNP309G/G}$ $p53^{515A/+}$, and $Mdm2^{SNP309T/T}$ $p53^{515A/+}$ Mice

	Genotype			
Tumor Type	$Mdm2^{SNP309G/G}$ (n = 5)	$Mdm2^{SNP309T/T}$ (n = 1)	$Mdm2^{SNP309G/G}$ $p53^{515A/+}$ (n = 48)	$Mdm2^{SNP309T/T}$ $p53^{515A/+}$ (n = 23)
Sarcoma	0	1	34	15
Fibrosarcoma	0	0	10	2
Leiomyosarcoma	0	0	1	0
Pleomorphic	0	0	2 (1)	0
Osteosarcoma	0	0	13 (2)	6 (1)
Histocytic	0	0	4	5
Spindle Cell	0	0	2 (1)	1
Histiocytoma	0	0	2	0
Ovarian hemangiosarcoma	0	0	1	0
Soft tissue sarcoma	0	1	1	2
Lipoma	0	0	2	1
Chondrosarcoma	0	0	1	0
Lymphoma	4	0	8	1
Adenoma				
Lung	0	0	1	0
Hepatocellular	0	0	1	0
Papilloma				
Squamous cell	0	0	1	0
Adenocarcinoma				
Mammary	1	0	3	0
Hepatocellular	0	0	1	2
Undefined	0	0	3	3
Carcinoma				
Salivary carcinoma	0	0	1 (1)	0
Squamous cell	1	0	2	1
Undefined	0	0	4	1
Total	6	1	64	24

Parentheses denote number of metastatic tumors.

Following the initial description of the $MDM2^{SNP309}$ allele, the actual impact of this SNP on human cancers has been confounded by conflicting reports vis-à-vis its impact on tumorigenesis in different tissues, ethnicity, or gender. In our study, significant differences in *Mdm2* levels were observed in some tissues but not others. Additionally, some of the mice that carry two $Mdm2^{SNP309G}$ alleles developed female cancers such as breast adenocarcinomas regardless of *p53* status. This is at variance with the findings observed in $Mdm2^{SNP309T/T}$ $p53^{515A/+}$ control mice, in which no breast tumors were observed. The development of breast cancer is highly unusual in C57Bl/6 mice, particularly in the absence of an accompanying p53 mutation. These data suggest there may indeed be tissue specific consequences resulting from the presence of two $Mdm2^{SNP309G}$ alleles. Previous studies have shown that forced expression of Mdm2 in murine mammary tissue resulted in increased proliferation and development of breast cancer (Lundgren et al., 1997). The finding that some of these C57Bl/6 mice that carry the $Mdm2^{SNP309G}$ allele also develop breast cancer indicates that even a slight elevation of Mdm2 may result in an increased breast cancer risk.

Our studies emphasize the fact that an ~2-fold increase in *Mdm2* in some tissues significantly increases cancer risk. In comparison, *Mdm2* haploinsufficiency (a 2-fold decrease) enhanced survival in several tumor models, further emphasizing the sensitivity of p53 regulation by Mdm2 (Alt et al., 2003; Mendrysa et al., 2006; Terzian et al., 2007). The presence of the $Mdm2^{SNP309G}$ allele alters the homeostasis of the Mdm2/p53 axis resulting in decreased basal steady state levels of p53. The most likely explanation is that Mdm2 has the ability to target p53 for degradation more efficiently than itself. The low steady state levels of p53 observed in these $Mdm2^{SNP309G/G}$ mice may have a significant impact on potential tumor formation, as cells from these tissues may have a greater propensity to give rise to a fully transformed cell in response to even minor genomic insults or mitogenic stimulation. Thus, slight perturbations (up or down) to the p53 pathway may significantly impact tumor formation, and perhaps, response to chemotherapy.

In addition to tumor formation, Mdm2 and p53 also regulate each other in response to DNA damage (Haupt et al., 1997; Kubbutat et al., 1997; Shieh et al., 1997; Siliciano et al., 1997). Loss of one *Mdm2* allele renders mice harboring wild-type *p53* sensitive

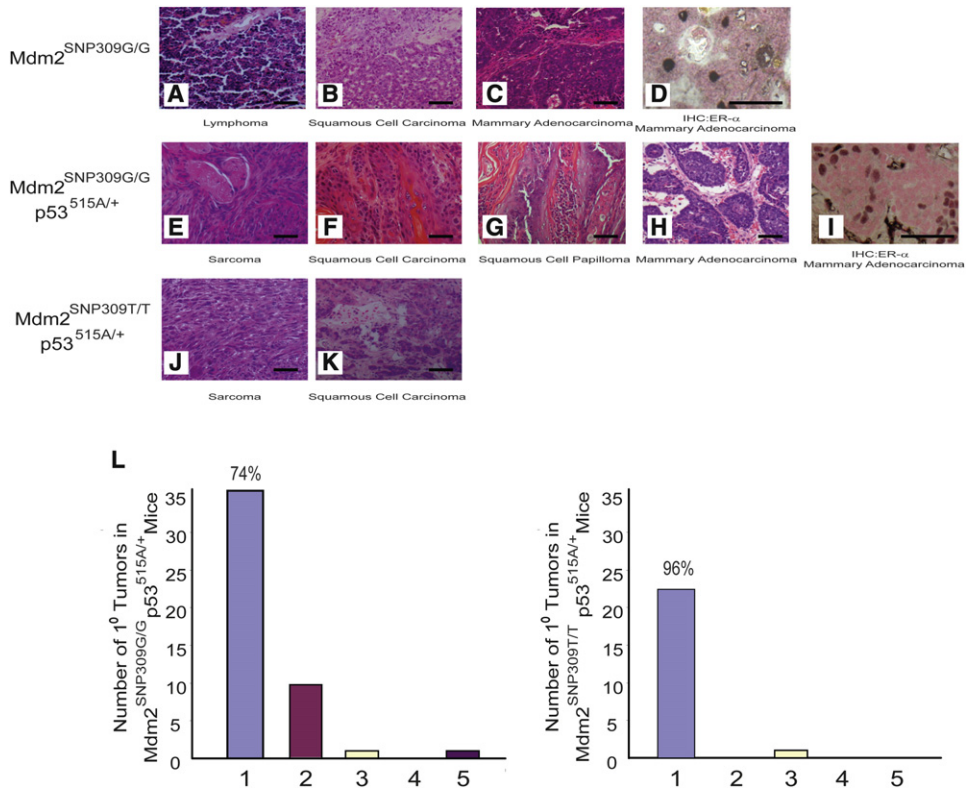

Figure 6. Mice Harboring Two *Mdm2*^{SNP309G} Alleles Express High Levels of Mdm2 and Develop a Unique Tumor Spectrum as Compared to Mice Harboring Two *Mdm2*^{SNP309T} Alleles

(A–C) Hematoxylin and eosin (H&E) staining of paraffin-embedded sections of tumors from *Mdm2*$^{SNP309G/G}$ mice. (A) Lymphoma. (B) Squamous cell carcinoma. (C) Mammary adenocarcinoma.

(D) Immunohistochemistry of estrogen receptor-α positive mammary adenocarcinoma from an *Mdm2*$^{SNP309G/G}$ mouse.

(E–H) H&E staining of paraffin-embedded sections of tumors from *Mdm2*$^{SNP309G/G}$ *p53*$^{515A/+}$ mice. (E) Sarcoma. (F) Squamous cell carcinoma. (G) Squamous cell papilloma. (H) Mammary adenocarcinoma.

(I) Immunohistochemistry of estrogen receptor-α positive mammary adenocarcinoma from an *Mdm2*$^{SNP309G/G}$ *p53*$^{515A/+}$ mouse.

(J and K) H&E staining of paraffin-embedded sections of tumors from *Mdm2*$^{SNP309T/T}$ *p53*$^{515A/+}$ mice. (J) Sarcoma. (K) Squamous cell carcinoma. The scale bar represents 50 μm in each figure.

(L) The graph depicts the number of primary tumors in *Mdm2*$^{SNP309G/G}$ *p53*$^{515A/+}$ and *Mdm2*$^{SNP309T/T}$ *p53*$^{515A/+}$ mice. The number above the bar represents the percentage of mice that had one primary tumor.

to p53-dependent toxicity after IR (Mendrysa et al., 2003; Terzian et al., 2007), further emphasizing the importance of Mdm2 dosage on p53-dependent phenotypes. Our finding that steady state levels of p53 are decreased, coupled with the findings that p53-dependent apoptosis and transactivation of p53 targets are lower in *Mdm2*$^{SNP309G/G}$ mice exposed to IR suggests that modest increases in Mdm2 levels can disrupt p53 stability and activity. It is noteworthy that p53 levels were similar in both *Mdm2*$^{SNP309G/G}$ and *Mdm2*$^{SNP309T/T}$ mice after IR, even though activation of p53 targets was ablated in the *Mdm2*$^{SNP309G/G}$ mice, suggesting that stabilization of p53 caused by ionizing radiation may overwhelm the destabilizing effects of the *Mdm2*^{SNP309G} allele on p53. It is therefore tempting to hypothesize that normal individuals harboring two *Mdm2*^{SNP309G} alleles may be more sensitive to exogenous low level DNA damage caused by environmental stress due to lower steady state p53 levels. A strength of this *Mdm2*^{SNP309G} mouse model herein reported is that it may aid in understanding the complex and fine-tuned interplay between variants of the p53 pathway (e.g., p53 mutations, Mdm2 SNPs), environmental stresses (e.g., carcinogens), response to chemotherapeutic agents, and tumor-independent variables (e.g., gender) in human cancer.

EXPERIMENTAL PROCEDURES

Generation of *Mdm2*$^{SNP309G/G}$ and *Mdm2*$^{SNP309T/T}$ Mice

A PCR-based strategy was used to generate a targeting vector containing the deletion of murine intron 1 with replacement by the human intron 1 harboring either the G or T nucleotide at position 309. To this end, the human intron 1 was cloned by PCR amplification of human genomic DNA using chimeric 5′-mouse-human-3′ forward and reverse primers. The forward primer contained 21 nucleotides upstream of the mouse exon 1-intron 1 junction. Three additional C nucleotides were added to the 5′ end of the forward primer to create a unique SmaI site. These three C nucleotides were deleted during blunt end digestion and thus resulted in no additions or alterations to the genome. The reverse 5′ murine-human 3′ primer contained 32 nucleotides of the mouse genome downstream of the mouse intron 1-exon 2 junction. Sequence analysis of the PCR product confirmed the presence of the G nucleotide at position 309 in the human *MDM2* intron 1 amplicon. The human *MDM2* intron 1 containing the T nucleotide was generated by site directed mutagenesis. The resulting

human *MDM2* intron 1 amplicons, possessing murine exon 1 and exon 2 ends, were used as reverse MEGAprimers along with forward primer 5′-CTAGC GACCATTGCGGTTTCGAG-3′ (~300 base pairs upstream of murine exon 1). This resulted in an amplicon containing murine exon 1, human intron 1, and a portion of murine exon 2. Next, we used PCR to generate a murine amplicon possessing the remainder of exon 2, intron 3, exon 3, a portion of intron 3, a *LoxP* site, and unique BamHI and SalI sites from a *pBSK*-based plasmid (B.11) containing genomic murine *Mdm2* ~6 Kb upstream and 2.5 Kb downstream of the first *ATG* in exon 3. Next, 5.7 kb of genomic DNA, upstream of exon 1, was digested from *pBSK-B.11*. Four piece ligation was used to generate the 5′ arm in the *pGL1*-targeting vector containing a *PGK*-neomycin and a thymidine kinase cassette. The 3′ arm was generated by PCR amplification of intron 3. Of importance, the start of the 3′ arm is precisely at the end of the 5′ arm. This arm contained a unique SalI site (destroyed during cloning), a *Lox P* site, 1 kb of intron 3, and a conserved *NheI* site. This amplicon was cloned immediately downstream of the neomycin cassette in the targeting vector. The resulting plasmids, containing the G or T alleles, were completely sequenced and contained no mutations. Both targeting constructs were linearized with *AscI* and electroporated into TC-1 embryonic stem (ES) cells. DNA from G418 and ganciclovir selected ES cells was isolated, digested by *SpeI*, and subjected to mini-Southern blot analysis using external 5′, 3′, and neomycin probes. Correctly targeted ES cells of the $Mdm2^{SNP309G}$ and $Mdm2^{SNP309T}$ were expanded and Southern blot analysis was repeated to confirm the integrity of the locus. These ES cell lines were used for injection into C57BL/6 blastocysts to generate chimeric mice. Male chimeric mice from each clone were crossed with C57BL/6 female mice and contributed to the germline of offspring mice. The resulting heterozygous mice were backcrossed two generations with C57Bl/6 mice, followed by one cross to C57Bl/6 females containing the *Zp3-cre* transgene. Female offspring were then further backcrossed two additional times to C57Bl/6 mice, followed by one cross to C57Bl/6 mice harboring the $p53^{515A}$ allele. These mice were then intercrossed to generate a cohort of heterozygous and homozygous mice for tumor studies. The background of all mice used in these studies is >96% C57Bl/6. For mouse embryonic fibroblasts, $Mdm2^{SNP309G/G}$ or $Mdm2^{SNP309T/T}$ mice were crossed and embryos were collected at 13.5 dpc. All animal studies were carried out according to M.D. Anderson Cancer Center and Institutional Animal Care and Use Committee Guidelines for Animal Use (IACUC) (protocol 079906634).

Genotyping Analysis

Tails from mice were genotyped for Mdm2 using forward primers 5′-GCATTA GAGAGTGGTCACTGCGAC-3′ and reverse primers 5′-GAACAGTGATAGAA CATCATGTCAC-3′ for the *Mdm2* alleles and previously described primers for the *p53* alleles (Jacks et al., 1994; Liu et al., 2004). In addition to PCR genotyping, tail DNA from $Mdm2^{SNP309G/G}$ and $Mdm2^{SNP309T/T}$ mice were randomly sequenced to confirm the presence of the G or T nucleotide after amplification using forward primer 5′-GGATTTCGGACGGCTCTCG-3′ and reverse primer 5′-CGCGCAGCGTTCACACTAG-3′. The resulting amplicons were sequenced using the forward primer.

Real-Time RT-PCR

Tissues and tumors were isolated from mice and RNA was extracted using TRIZOL, followed by DNAaseI treatment. RNA from early passage MEFs (<P2) was extracted as above. First strand synthesis was carried out per the manufacturer's protocol (GE Bioscience) on total RNA isolated from each tissue. The resulting first strand DNA was amplified in the RT-PCR using primers for *Mdm2* (forward 5′-GAAAAGCCTGAGGCTGGTAGAA-3′ and reverse 5′-AACATAGGCAACCACCAGGAA-3′), *Rplp0* (forward 5′-CCCT GAAGTGCTCGACATCA-3′ and reverse 5′-TGCGGACACCCTCCAGAA-3′), *Puma* (forward 5′-GCGGCGGAGACAAGAAGA-3′ and reverse 5′-AGTCCCA TGAAGAGATTGTACATGAC-3′), *Perp* (forward 5′-GCTGCAGCCACGCTTTTC and reverse 5′-GGCGAAGAACGAGAGAATGAA-3′), *Ccng1* (forward 5′-GCG AAGCATCTTGGGTGTGT-3′ and reverse 5′-TCCTTTCCTCTTCAGTCGCT TT-3), and *Pig8* (forward 5′-GGCATCTGTACCATCTCAAAGCT-3′ and reverse 5′-TCGACGCTGTTCCTCTCTCTTC-3′). The RT-PCR primers for *p21* have been previously described (Post et al., 2010). Expression of mRNA was normalized to expression of *Rplp0* in each reaction.

RNase Protection Assay

Total RNA from spleens of different mice were hybridized with a ^{32}P radiolabeled antisense Exon 1–3 *Mdm2* probe followed by incubation with RNase A. The RNA-^{32}P probe complex was resolved on a 5% polyacrylmide gel, transferred to Whatman paper, and dried. The gel was then exposed on Bio-Max XRay film.

Cell Culture of MEFs

Early passage MEFs were grown in DMEM supplemented with 15% FCS and 1% penicillin/streptomycin. MEFs were either untreated or treated with 500 nM mithramycin A (Sigma) for 18 hr and then harvested.

Cell Proliferation Assays

Three separate $Mdm2^{SNP309G/G}$ and $Mdm2^{SNP309T/T}$ passage 2 MEF cell lines were plated at 15,000 cells per triplicate well in a 24-well plate. MTT assay [3-(4,5-dimethylthiazol-2-yl)-2,5-diphenyl tetrazolium bromide] was carried out on days 1, 3, and 5 as previously published (Jackson et al., 1998). Absorbance values were averaged for the triplicate wells for each cell line, and then the three individual cell lines were grouped and averaged with error bars representing standard error of the mean.

Immunoblotting Analysis

Spleens, thymi, breast, tumors, and MEFs were collected and frozen in liquid nitrogen. Protein extracts were prepared by homogenizing the tissues or cells in NP-40 lysis buffer supplemented with Complete Protease (Roche) and phosphatase inhibitors. Soluble proteins were boiled in 2×-SDS-sample buffer, separated by SDS-PAGE, and transferred to PVDF membranes (Millipore). Membranes were incubated with rabbit α-p53 (CM5) (Vector Laboratory), mouse α-Mdm2 (2A10) (Calbiochem), rabbit α-phospho-Ser18p53 (Cell Signaling), mouse α-β-actin (Sigma), or mouse α-vinculin (Sigma) antibodies and antigen-antibody complexes were detected by the enhanced chemiluminescence Kit (GE Bioscience) or BCIP/NBT Color Development Substrate (Promega). Determination of band intensity in western blots was carried out using ImageQuant software (GE Healthcare).

Gamma Irradiation and Thymic Apoptosis Assays

Six-week-old mice were treated with 1 Gy IR and sacrificed 3 hr posttreatment. Tissues were harvested and frozen in liquid nitrogen. Western blot analysis was carried out as above. For apoptotic assays, thymi were harvested and fixed in 10% phosphate buffered formalin (Sigma) followed by paraffin embedding. Serial sections were either stained with hematoxylin and eosin (H&E) or subjected to immunohistochemistry (IHC). For IHC, sections were deparaffinized and antigens were retrieved using citric acid and steam. IHC was carried out using rabbit α-cleaved caspase-3 (Cell Signaling) and visualized by ABC and DAB kits (Vector Laboratories). Slides were counterstained with Nuclear Fast Red.

Pathological Analysis of Tumors

Moribund mice were sacrificed according to M.D. Anderson Cancer Center and IACUC guidelines. Euthanized mice were necropsied and tissues were harvested and fixed in 10% phosphate buffered formalin followed by paraffin embedding. Tissue sections were stained with hematoxylin and eosin and morphologic analysis was carried out by the Department of Veterinary Medicine at M.D. Anderson Cancer Center. For IHC, sections were deparaffinized and antigens were retrieved using citric acid and steam. IHC was carried out using or rabbit α-Mdm2 (R & D Systems) and visualized by ABC and DAB kits. Slides were counterstained with Nuclear Fast Red. Breast tumors were confirmed by immunohistochemistry as above using mouse α-estrogen receptor-α, 1D5 (Dako).

Sequence Analysis

Loss of heterozygosity at the *p53* locus was determined by PCR amplification of genomic tumor DNA using forward primer 5′–TACTCT-CCTCCCCTCAA TAAGCTATTC-3′ (exon 5) and reverse primer 5′-AGTCCTAACCCCACAG GCGGTGTT-3′ (intron 5). The PCR amplicons were then sequencing using the exon 5 primer and analyzed using Chromas software.

Statistical Analysis

Comparisons of mean values between the groups were analyzed using GraphPad Instat software (GraphPad Software Inc.). Statistical significance of the differences was analyzed by using unpaired Student's t test for comparisons of two groups, ANOVA for comparisons of more than two groups, or the χ^2 test for 2 by 2 comparisons. Survival curves were plotted by the Kaplan-Meier method and compared by the log rank (Mantel-Cox) test using GraphPad Prism. All p values were two-sided and the level of statistical significance was set at <0.05.

SUPPLEMENTAL INFORMATION

Supplemental Information includes four figures and can be found with this article online at doi:10.1016/j.ccr.2010.07.010.

ACKNOWLEDGMENTS

We thank members of the Lozano lab for helpful discussion and technical advice. DNA sequencing and veterinary core facilities were supported by an NCI Cancer Center Support (grant CA16672). S.M.P. was supported by a Ruth L. Kirschstein NRSA fellowship (F32CA119616) and is a recipient of the Dowdy P. Hawn postdoctoral fellowship. J.G.J. was funded as an Odyssey Scholar and supported by the Odyssey Program and The Theodore N. Law Endowment for Scientific Achievement. This study has been supported by National Institutes of Health (CA46392 and CA34936 to G.L.; ES015587 and ES011047 to D.G.J.) and the Cancer Prevention Institute of Texas.

Received: January 25, 2010
Revised: May 21, 2010
Accepted: July 20, 2010
Published: September 13, 2010

REFERENCES

Alt, J.R., Greiner, T.C., Cleveland, J.L., and Eischen, C.M. (2003). Mdm2 haploinsufficiency profoundly inhibits Myc-induced lymphomagenesis. EMBO J. *22*, 1442–1450.

Alvarez, S., Drane, P., Meiller, A., Bras, M., Deguin-Chambon, V., Bouvard, V., and May, E. (2006). A comprehensive study of p53 transcriptional activity in thymus and spleen of gamma irradiated mouse: high sensitivity of genes involved in the two main apoptotic pathways. Int. J. Radiat. Biol. *82*, 761–770.

Bond, G.L., Hirshfield, K.M., Kirchhoff, T., Alexe, G., Bond, E.E., Robins, H., Bartel, F., Taubert, H., Wuerl, P., Hait, W., et al. (2006). MDM2 SNP309 accelerates tumor formation in a gender-specific and hormone-dependent manner. Cancer Res. *66*, 5104–5110.

Bond, G.L., Hu, W., Bond, E.E., Robins, H., Lutzker, S.G., Arva, N.C., Bargonetti, J., Bartel, F., Taubert, H., Wuerl, P., et al. (2004). A single nucleotide polymorphism in the MDM2 promoter attenuates the p53 tumor suppressor pathway and accelerates tumor formation in humans. Cell *119*, 591–602.

Bond, G.L., and Levine, A.J. (2007). A single nucleotide polymorphism in the p53 pathway interacts with gender, environmental stresses and tumor genetics to influence cancer in humans. Oncogene *26*, 1317–1323.

Bougeard, G., Baert-Desurmont, S., Tournier, I., Vasseur, S., Martin, C., Brugieres, L., Chompret, A., Bressac-de Paillerets, B., Stoppa-Lyonnet, D., Bonaiti-Pellie, C., and Frebourg, T. (2006). Impact of the MDM2 SNP309 and p53 Arg72Pro polymorphism on age of tumour onset in Li-Fraumeni syndrome. J. Med. Genet. *43*, 531–533.

Chien, W.-P., Wong, R.-H., Cheng, Y.-W., Chen, C.-Y., and Lee, H. (2010). Associations of MDM2 SNP309, transcriptional activity, mRNA expression, and survival in stage I non-small-cell lung cancer patients with wild-type p53 tumors. Ann. Surg. Oncol. *17*, 1194–1202.

Copson, E.R., White, H.E., Blaydes, J.P., Robinson, D.O., Johnson, P.W., and Eccles, D.M. (2006). Influence of the MDM2 single nucleotide polymorphism SNP309 on tumour development in BRCA1 mutation carriers. BMC Cancer *6*, 80.

Dharel, N., Kato, N., Muroyama, R., Moriyama, M., Shao, R.X., Kawabe, T., and Omata, M. (2006). MDM2 promoter SNP309 is associated with the risk of hepatocellular carcinoma in patients with chronic hepatitis C. Clin. Cancer Res. *12*, 4867–4871.

Donehower, L.A., and Lozano, G. (2009). 20 years studying p53 functions in genetically engineered mice. Nat. Rev. Cancer *9*, 831–841.

Economopoulos, K.P., and Sergentanis, T.N. (2009). Differential effects of MDM2 SNP309 polymorphism on breast cancer risk along with race: a meta-analysis. Breast Cancer Res. Treat. *120*, 211–216.

Ellis, N.A., Huo, D., Yildiz, O., Worrillow, L.J., Banerjee, M., Le Beau, M.M., Larson, R.A., Allan, J.M., and Onel, K. (2008). MDM2 SNP309 and TP53 Arg72Pro interact to alter therapy-related acute myeloid leukemia susceptibility. Blood *112*, 741–749.

Grochola, L.F., Müller, T.H., Bond, G.L., Taubert, H., Udelnow, A., and Würl, P. (2010). MDM2 SNP309 associates with accelerated pancreatic adenocarcinoma formation. Pancreas *39*, 76–80.

Haupt, Y., Maya, R., Kazaz, A., and Oren, M. (1997). Mdm2 promotes the rapid degradation of p53. Nature *387*, 296–299.

Iwakuma, T., and Lozano, G. (2003). MDM2, an introduction. Mol. Cancer Res. *1*, 993–1000.

Jacks, T., Remington, L., Williams, B.O., Schmitt, E.M., Halachmi, S., Bronson, R.T., and Weinberg, R.A. (1994). Tumor spectrum analysis in p53-mutant mice. Curr. Biol. *4*, 1–7.

Jackson, J.G., White, M.F., and Yee, D. (1998). Insulin receptor substrate-1 is the predominant signaling molecule activated by insulin-like growth factor-I, insulin, and interleukin-4 in estrogen receptor-positive human breast cancer cells. J. Biol. Chem. *273*, 9994–10003.

Krekac, D., Brozkova, K., Knoflickova, D., Hrstka, R., Muller, P., Nenutil, R., and Vojtesek, B. (2008). MDM2 SNP309 does not associate with elevated MDM2 protein expression or breast cancer risk. Oncology *74*, 84–87.

Kubbutat, M.H., Jones, S.N., and Vousden, K.H. (1997). Regulation of p53 stability by Mdm2. Nature *387*, 299–303.

Lang, G.A., Iwakuma, T., Suh, Y.A., Liu, G., Rao, V.A., Parant, J.M., Valentin-Vega, Y.A., Terzian, T., Caldwell, L.C., Strong, L.C., et al. (2004). Gain of function of a p53 hot spot mutation in a mouse model of Li-Fraumeni syndrome. Cell *119*, 861–872.

Liu, G., Parant, J.M., Lang, G., Chau, P., Chavez-Reyes, A., El-Naggar, A.K., Multani, A., Chang, S., and Lozano, G. (2004). Chromosome stability, in the absence of apoptosis, is critical for suppression of tumorigenesis in Trp53 mutant mice. Nat. Genet. *36*, 63–68.

Lundgren, K., Montes de Oca Luna, R., McNeill, Y.B., Emerick, E.P., Spencer, B., Barfield, C.R., Lozano, G., Rosenberg, M.P., and Finlay, C.A. (1997). Targeted expression of MDM2 uncouples S phase from mitosis and inhibits mammary gland development independent of p53. Genes Dev. *11*, 714–725.

Marcel, V., Palmero, E.I., Falagan-Lotsch, P., Martel-Planche, G., Ashton-Prolla, P., Olivier, M., Brentani, R.R., Hainaut, P., and Achatz, M.I. (2009). TP53 PIN3 and MDM2 SNP309 polymorphisms as genetic modifiers in the Li-Fraumeni syndrome: impact on age at first diagnosis. J. Med. Genet. *46*, 766–772.

Mendrysa, S.M., McElwee, M.K., Michalowski, J., O'Leary, K.A., Young, K.M., and Perry, M.E. (2003). MDM2 is critical for inhibition of p53 during lymphopoiesis and the response to ionizing irradiation. Mol. Cell. Biol. *23*, 462–472.

Mendrysa, S.M., O'Leary, K.A., McElwee, M.K., Michalowski, J., Eisenman, R.N., Powell, D.A., and Perry, M.E. (2006). Tumor suppression and normal aging in mice with constitutively high p53 activity. Genes Dev. *20*, 16–21.

Menin, C., Scaini, M.C., De Salvo, G.L., Biscuola, M., Quaggio, M., Esposito, G., Belluco, C., Montagna, M., Agata, S., D'Andrea, E., et al. (2006). Association between MDM2-SNP309 and age at colorectal cancer diagnosis according to p53 mutation status. J. Natl. Cancer Inst. *98*, 285–288.

Oliner, J.D., Kinzler, K.W., Meltzer, P.S., George, D.L., and Vogelstein, B. (1992). Amplification of a gene encoding a p53-associated protein in human sarcomas. Nature *358*, 80–83.

Post, S.M., Quintas-Cardama, A., Terzian, T., Smith, C., Eischen, C.M., and Lozano, G. (2010). p53-dependent senescence delays Emu-myc-induced B-cell lymphomagenesis. Oncogene *29*, 1260–1269.

Ruijs, M.W., Schmidt, M.K., Nevanlinna, H., Tommiska, J., Aittomaki, K., Pruntel, R., Verhoef, S., and Van't Veer, L.J. (2007). The single-nucleotide polymorphism 309 in the MDM2 gene contributes to the Li-Fraumeni syndrome and related phenotypes. Eur. J. Hum. Genet. *15*, 110–114.

Khan, S.A., Idrees, K., Forslund, A., Zeng, Z., Rosenberg, S., Pincas, H., Barany, F., Offit, K., Laquaglia, M.P., and Paty, P.B. (2008). Genetic variants in germline TP53 and MDM2 SNP309 are not associated with early onset colorectal cancer. J. Surg. Oncol. *97*, 621–625.

Schmidt, M.K., Reincke, S., Broeks, A., Braaf, L.M., Hogervorst, F.B., Tollenaar, R.A., Johnson, N., Fletcher, O., Peto, J., Tommiska, J., et al. (2007). Do MDM2 SNP309 and TP53 R72P interact in breast cancer susceptibility? A large pooled series from the breast cancer association consortium. Cancer Res. *67*, 9584–9590.

Shieh, S.Y., Ikeda, M., Taya, Y., and Prives, C. (1997). DNA damage-induced phosphorylation of p53 alleviates inhibition by MDM2. Cell *91*, 325–334.

Siliciano, J.D., Canman, C.E., Taya, Y., Sakaguchi, K., Appella, E., and Kastan, M.B. (1997). DNA damage induces phosphorylation of the amino terminus of p53. Genes Dev. *11*, 3471–3481.

Soussi, T., and Lozano, G. (2005). p53 mutation heterogeneity in cancer. Biochem. Biophys. Res. Commun. *331*, 834–842.

Tabori, U., Nanda, S., Druker, H., Lees, J., and Malkin, D. (2007). Younger age of cancer initiation is associated with shorter telomere length in Li-Fraumeni syndrome. Cancer Res. *67*, 1415–1418.

Terzian, T., Wang, Y., Van Pelt, C.S., Box, N.F., Travis, E.L., and Lozano, G. (2007). Haploinsufficiency of Mdm2 and Mdm4 in tumorigenesis and development. Mol. Cell. Biol. *27*, 5479–5485.

Valentin-Vega, Y.A., Barboza, J.A., Chau, G.P., El-Naggar, A.K., and Lozano, G. (2007). High levels of the p53 inhibitor MDM4 in head and neck squamous carcinomas. Hum. Pathol. *38*, 1553–1562.

Venter, J.C., Adams, M.D., Myers, E.W., Li, P.W., Mural, R.J., Sutton, G.G., Smith, H.O., Yandell, M., Evans, C.A., Holt, R.A., et al. (2001). The sequence of the human genome. Science *291*, 1304–1351.

Vogelstein, B., Lane, D., and Levine, A.J. (2000). Surfing the p53 network. Nature *408*, 307–310.

Yarden, R.I., Friedman, E., Metsuyanim, S., Olender, T., Ben-Asher, E., and Papa, M.Z. (2008). MDM2 SNP309 accelerates breast and ovarian carcinogenesis in BRCA1 and BRCA2 carriers of Jewish-Ashkenazi descent. Breast Cancer Res. Treat. *111*, 497–504.